Experimental Demonstration of Nondisruptive, Central Fueling of a Tokamak by Compact Toroid Injection

R. Raman,* F. Martin,† B. Quirion,‡ M. St-Onge,§ J-L. Lachambre,‖ D. Michaud,§ B. Sawatzky,¶ J. Thomas,** A. Hirose,†† D. Hwang,** N. Richard,§ C. Côté,‖ G. Abel,† D. Pinsonneault,† J-L. Gauvreau,† B. Stansfield,† R. Décoste,‖ A. Côté,‖ W. Zuzak,† and C. Boucher†

Centre Canadien de Fusion Magnétique, Varennes, Québec, Canada J3X 1S1

(Received 22 June 1994)

We report the first results of nondisruptive, central fueling of a tokamak by the injection of an accelerated spheromak compact toroid (CT). Interferometry measurements indicate central fueling of the tokamak plasma on a fast time scale (<0.5 ms), with more than 50% of the CT mass used for plasma fueling. The tokamak particle inventory increased by more than 30% without disruption.

PACS numbers: 52.55.Hc, 52.55.Fa, 52.75.Di

On-line particle fueling is needed for long-pulse or steady state operation of a tokamak. Present fueling schemes such as gas puffing and pellet injection are not considered adequate to fuel the center of reactor tokamak plasmas. Fuel deposited in the edge by such schemes will be transported to the center by diffusion processes. However, a large portion of the fuel will not reach the center and will be lost before burnup. Thus present reactor design studies utilizing these fueling methods assume only 5% burnup of the injected fuel. With a large tritium recycle fraction in the fuel cycle, undesirable amounts of tritium may accumulate on the vessel walls and limit reactor lifetime. Central penetration of the injected fuel is important to maximize tritium burnup, to reduce tritium inventory in the fuel cycle, to reduce tritium accumulation in the vessel walls, and for density profile control of the tokamak. While neutral beams have been used on a limited scale, they are too inefficient for fueling purposes.

Perkins *et al.* [1], Parks [2], and Newcomb [3] proposed the use of accelerated spheromak compact toroids for central fueling of tokamak plasmas. The spheromak is a compact toroid (CT) plasma configuration with approximately equal toroidal and poloidal magnetic fields [4]. It can be formed in a magnetized Marshall gun [5,6] and efficiently accelerated to high velocities [7,8]. Central fueling of a reactor requires injection velocities in the range of 350 to 800 km/s which can be achieved only by accelerated CTs. A previous injection experiment using a relatively large nonaccelerated CT (CALTECH device: CT velocity = 30 km/s, CT diameter = 8 cm) into the small, low field, and relatively cold ENCORE tokamak (R = 38 cm, a = 12 cm, I_p = 2 kA, B_T = 0.07 T, $T_e \sim$ 12 eV, 1 ms discharge) resulted in a tenfold increase in the tokamak particle inventory and a quenching of the tokamak discharge [9,10].

We have performed CT injection experiments using the CTF device (Compact Toroid Fueler) into the TdeV tokamak. We present the first experimental results of nondisruptive, central fueling of a tokamak by accelerated CT spheromak injection. Measurements indicate that most of the CT mass is used for fueling the tokamak. CT injection successfully increased the particle inventory of the TdeV tokamak by more than 30%. Multichord interferometer signals show central penetration for toroidal fields (B_T) of 0.73, 0.84, and 1.0 T. Partial penetration of the tokamak discharge (~30% minor radius) is observed for B_T = 1.5 T.

The experimental configuration is shown in Fig. 1. In CTF the spheromak is initially formed and contained in a precompression region. An externally induced radial current sheath accelerates the CT to high velocity by the $\mathbf{J} \times \mathbf{B}$ force. Since the spheromak plasma is confined by self-contained magnetic fields, most of the mass is retained within the elongated spheromak configuration during the acceleration process. In CTF, two diagnostic ports located 65 cm apart on the accelerator section contain poloidal magnetic probes that measure the CT surface magnetic field as the CT translates past them [11]. The time delay between these signals is used to determine the average velocity of the CT during acceleration which for these experiments ranges from 120 to 220 km/s. Since measurements are made at only two locations, the final velocity of the CT cannot be determined. A He-Ne interferometer located at the diagnostic port near the focus cone is used to determine the CT density. The CT length calculated using the average velocity and the FWHM of the density signal is between 20 and 50 cm. The CT diameter is limited by the accelerator diameter to 14 cm. The CT density in the accelerator ranges from 1×10^{21} to 7×10^{21} m^{-3} with a corresponding mass between 10 and 60 μg. In CTF there is a final compression in the focus cone to a diameter of 9 cm. The final length is anticipated to be between 12 and 30 cm due to self-similar compression of the CT, resulting in a factor of 3 increase in the CT density. CT self-similar compression has been observed on the RACE device [12] using a tapered accelerator electrode where the CT length decreased in proportion to its radius.

The CT is injected into the TdeV tokamak [13], a medium sized machine with a major and a minor radius

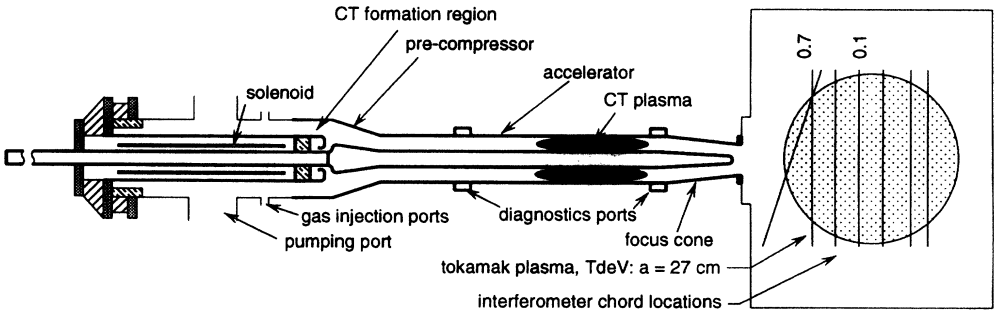

FIG. 1. Schematic of the experimental setup showing the CT injector in relation to the tokamak. The vertical lines overlaid on the tokamak cross section show the location of the interferometer beams. The $r/a = 0.1$ and 0.7 chords are located as shown in the figure.

of $R = 86$ cm and $a = 27$ cm, respectively. For these experiments the tokamak was operated with a toroidal field of 0.73 to 1.0 T and a plasma current between 100 and 120 kA for a corresponding edge q between 4 and 6. The central q is always greater than 1. The plasma is Ohmically heated and operated in a double null poloidal divertor configuration. The electron density is in the range of $(1-2) \times 10^{19}$ m^{-3} with a corresponding nominal particle inventory of $(1.3-2.6) \times 10^{19}$ ions. CT injection can provide between 30% and 90% fueling for these plasmas. The feedback controlled tokamak gas injection used to maintain a constant electron density is interrupted 2 ms before CT injection, preventing gas injection for the rest of the discharge. In these experiments a D^+ or H^+ CT was injected into a tokamak plasma of the same isotope.

Diagnostic traces for a typical tokamak discharge with central penetration of the CT are shown in Fig. 2. There is no disruption following CT injection at 602 ms. The central ($r/a = 0.1$) and outer ($r/a = 0.7$) interferometer chords show a fast rising (<0.5 ms) density from CT fueling followed by a slower decrease. The measured 2–3 ms e-folding time of the density decay is consistent with the estimated particle confinement time for these low field, low temperature discharges. Post-CT fueling ($t > 604$ ms) increases the tokamak density again to the density limit, causing a loss of central density about 70 ms after CT injection. For CT injection into a low density tokamak plasma ($\sim 1 \times 10^{19}$ m^{-3}), the post-CT fueling related density buildup never reaches the density limit. Several sources can contribute to post-CT edge fueling of the tokamak plasma: the diffuse plasma trailing the CT, gas used for CT formation which has not been ionized, and increased recycling from the tokamak walls due to increased particle losses after CT injection. The mass of the trailing plasma generally exceeds the CT mass, while the unused portion of the CT formation gas typically represents >100% of the tokamak particle inventory. In this Letter, we restrict our discussion of the fast time scale CT specific fueling.

Shortly after CT injection, when the magnetohydrodynamic (MHD) oscillations have built up to high levels, we generally observe a sudden drop in the central soft x-ray signal and an increase in the H_α signal. Thomson scattering measurements made within 100 to 400 μs after CT injection indicate a strong cooling of the central plasma (600 to <400 eV); this low value of T_e is an upper limit since the central Thomson scattering channel is optimized to measure $T_e > 400$ eV. This decrease in T_e is responsible for the drop in the soft x-ray signal from the $\exp(-E_\nu/T_e)$ dependence, where E_ν is the mean energy of the sampled x rays. The associated increase in resistivity causes the loop voltage (V_L) to increase and the plasma current (I_p) to decrease. This decrease in electron temperature could be caused by impurities contained in the CT plasma and by the large addition of cold plasma. Oxygen and carbon lines have been observed in CTF but the absolute level of these and metallic impurities is unknown. Reduction in temperature could also be caused by enhanced electron thermal conductivity (χ_e) resulting from high levels of MHD

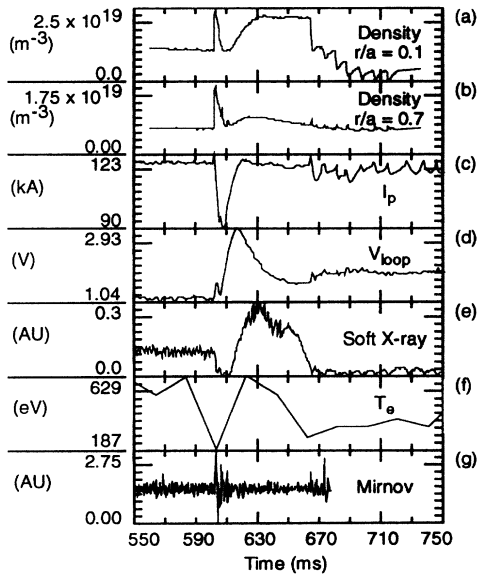

FIG. 2. Time history of tokamak parameters for the central penetration case at $B_T = 1$ T: (a) line averaged electron density at $r/a = 0.1$, (b) line averaged electron density at $r/a = 0.7$, (c) plasma current (I_p), (d) loop voltage (V_L), (e) central chord soft x-ray signal, (f) Thomson scattering electron temperature in the plasma center, and (g) Mirnov coil signal.

oscillations [14]. The electron temperature recovers within about 10 to 20 ms of CT injection.

Strong MHD oscillation occurring about 0.5 ms or more after CT injection (Mirnov signal) is dominated by the $m = 2$, $n = 1$ mode. On some shots we observe a conversion to higher poloidal mode numbers correlated with a rapid (<0.5 ms) decrease in the density signal from the centermost ($r/a = 0.1$) interferometer chords and a simultaneous increase on the outer ($r/a > 0.5$) interferometer chords, indicating a rapid transfer of particles from the inner to the outer flux surfaces. The onset of these modes is possibly caused by the large perturbation to the particle inventory and the resulting response of the tokamak to redistribute the injected fuel.

A CT injected into a tokamak will slow down due to the toroidal field gradient [1]. CT penetration into the tokamak requires that the CT kinetic energy density exceed the displaced toroidal field energy density ($0.5\rho v^2 > B_T^2/2\mu_0$), where ρ and v are the CT mass density and velocity and B_T is the tokamak toroidal field. Within the tokamak the CT will expand or contract to maintain pressure balance with the external plasma and magnetic pressure until it disintegrates. Two disintegration mechanisms were proposed by Parks [2]. In the first scheme the CT magnetic field is annihilated by dissipative magnetic merging processes occurring in a thin field reversal layer on the surface of the CT, resulting in a maximum CT lifetime of <5 μs for this experiment. In the second mechanism, resistive decay of the internal CT magnetic field is followed by a recompression of the CT until the density increases to a point where a critical β is reached, causing the CT to break up. The maximum resistive dissipation time scale for the present case is 100 μs. Both dissipation times are shorter than the time scale of events reported here.

For the partial penetration case of injection into a tokamak toroidal field of $B_T = 1.5$ T, $I_p = 210$ kA, we observe a sharp rise on the outermost interferometer chords ($r/a = 0.7, 0.9$) with a factor of 1.3 increase in density in ~0.5 ms [Fig. 3(a)]. This rate of density rise is longer than the CT dissipation time constant and consistent with the time necessary for injected particles to equilibrate on field lines. Chords located at $r/a < 0.7$ show a much slower rise in density indicative of inward diffusion from the outer flux surfaces (the central chord at $r/a = 0.1$ takes about 12 ms to peak). In comparison, for the central penetration case at $B_T = 1$ T [Fig. 3(b)], we see that all chords show a rapid increase in density. The tokamak particle inventory increased by a factor of 1.8. When only the CT gas valves are pulsed we do not see any measurable increase in the tokamak inventory during the first two ms after pulsing the valves, which is the time required for the CT gas to diffuse into the tokamak. After 2 ms, the rate of rise of the central density, for the case of gas puffing, is much less than for the partial penetration case shown in Fig. 3(a). Injection of a CT with low kinetic energy density (compared to the tokamak toroidal field energy density) or a poorly formed and accelerated CT results in edge fueling where

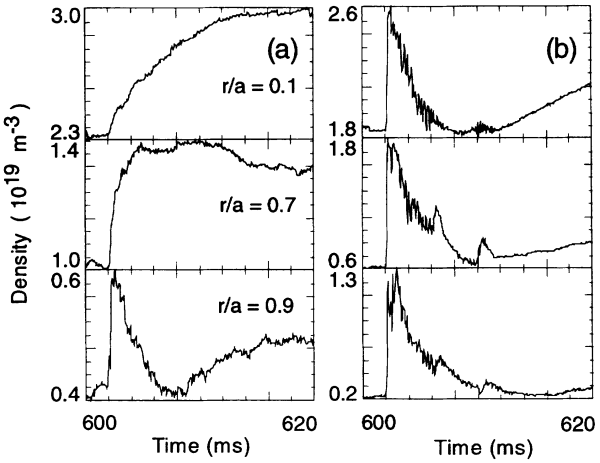

FIG. 3. Comparison of the rate of line averaged electron density increase for the case of (a) partial CT penetration at $B_T = 1.5$ T and (b) central penetration at $B_T = 1.0$ T. The CT is injected at 602.05 ms.

a sharp density increase is observed only in the outermost interferometer chord located at $r/a = 0.9$.

One can determine the depth of CT penetration by identifying the innermost interferometer chord signal that does not show any further increase in density after about 0.5 ms past the CT injection time. In general, on many of the shots with partial penetration, some of the CT fuel appears to reach the tokamak center on these time scales, but the tokamak inventory continues to increase for the next 0.5 to 1 ms, and longer still for edge fueling, as plasma diffuses inward. Because of the relatively long CT length (12 to 30 cm) compared to the TdeV minor radius (27 cm), the CT fuel is expected to be deposited over a large radial distance within the tokamak, producing a fast density increase on several interferometer chords after CT injection. For partial penetration of the longest CTs (length > 20 cm), not all the mass contained in the CT will be deposited within the tokamak, as part of the CT could extend beyond the last closed flux surface, contibuting to post-CT fueling. In Fig. 4 we plot the tokamak toroidal field energy density ($B_T^2/2\mu_0$) at the radial location up to which the CT has penetrated versus the CT kinetic energy density ($\rho v^2/2$). Here ρ is the CT plasma density after compression by the focus cone and v is the average CT velocity. Scaling of the tokamak toroidal field energy density at the point of maximum penetration is roughly linear with the CT kinetic energy density in agreement with the penetration model proposed by Perkins *et al.*, Parks, and Newcomb. The detailed scaling relations for CT slowing down and tilting cannot be verified from these measurements.

Figure 5 shows a plot of the increase in the tokamak particle inventory on a short time scale (~0.5 ms) versus the calculated mass of the CT. This short time scale is used to avoid contribution from post-CT fueling sources. The increase in the tokamak mass is greater than 50% of the CT mass indicating good CT fuel deposition. The

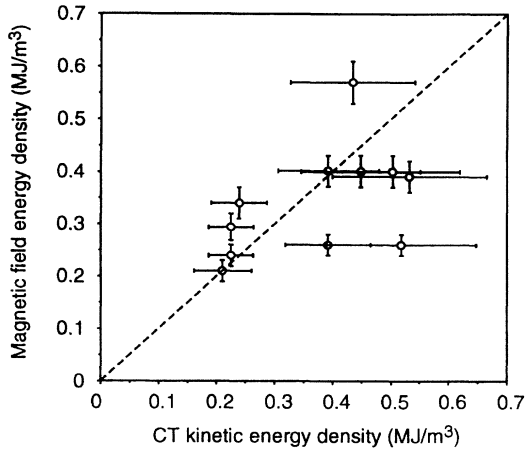

FIG. 4. Tokamak magnetic field energy density versus CT kinetic energy density based on average velocity. The dotted line represents the simplest CT penetration model.

fact that most of the fuel is deposited within the tokamak plasma is consistent with the estimated short dissociation time indicating that the CT does not bounce back [2].

In summary, we have experimentally demonstrated central fueling of a medium sized tokamak discharge by CT-spheromak injection. In these experiments the tokamak particle inventory was increased by a large fraction (>30%), without disruptions. Most of the CT fuel is deposited within the tokamak and there is no evidence of the CT bouncing back. The amount of impurities contained in the CT plasma was not quantified, but was not sufficient to push the Z_{eff} in the TdeV beyond the limit for tokamak disruption. A calculation of Z_{eff} based on plasma parameters indicates that the relative Z_{eff} increased by less than 20% after CT injection (for $t > t_{\text{CT}} + 20$ ms). Since the typical fueling per pulse for reactors is anticipated to be on the order of ~0.5% (compared to the present >30% at TdeV), much less perturbation to the tokamak should result after CT fueling under reactor conditions. A reactor tritium fueler operating at a compressed CT density of 5×10^{22} m^{-3} will require a CT velocity of ~350 km/s; these conditions should be attainable on a larger device [7,8]. Since the ratio $v_{\text{Alfvén-tok}}/v_{\text{CT}}$ will remain about the same as one scales to reactor sized devices, we do not expect the primary CT penetration and dissipation mechanisms to change. Post-CT fueling can be significantly decreased by optimization of gun design and greater vacuum pumping on the CT gun. That the tokamak mass can be nondisruptively increased by such large fractions is encouraging for the viability of the CT fueling concept.

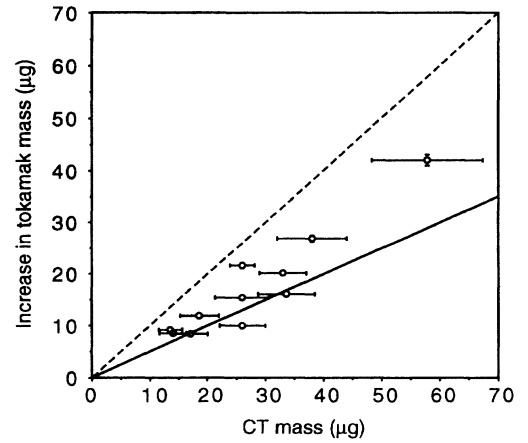

FIG. 5. Increase in the mass of the tokamak after CT injection versus the CT mass. The dotted line is the 100% fueling line and the solid line is the 50% fueling line.

We would like to acknowledge the continuous support of Dr. P. Gierszewski and the technical assistance of P. Nöel, M. Gagné, S. Paquin, S. Savoie, G. Bouchard, and L. Godbout for assistance in tokamak and diagnostics operation. The CTF project is funded by the Canadian Fusion Fuels Technology Project. We give special thanks to Dr. C. Daughney and Dr. B.C. Gregory for suggesting improvements to this document. The Centre Canadien de Fusion Magnétique is funded by Atomic Energy of Canada Limited, Hydro-Québec, and the Institut National de la Recherche Scientifique.

*Permanent address: Canadian Fusion Fuels Technology Project, Mississauga, Ontario, Canada L5J 1K3.
†Also at INRS-Energie et Matériaux, Varennes, Québec, Canada.
‡Also at DECATRON, St-Bruno, Québec, Canada.
§Also at MPB Technologies Inc., Dorval, Québec, Canada.
‖Also at Hydro-Québec, Varennes, Québec, Canada.
¶Permanent address: Department of Physics, University of Saskatchewan, Saskatoon, Saskatchewan, Canada S7N 0W0.
**Permanent address: Department of Applied Science, University of California–Davis, Livermore, CA, 94550.
††Permanent address: Department of Physics and Engineering Physics, University of Saskatchewan, Saskatoon, Saskatchewan, Canada S7N 0W0.

[1] L.J. Perkins *et al.*, Nucl. Fusion **28**, 1365 (1988).
[2] P.B. Parks, Phys. Rev. Lett. **61**, 1364 (1988).
[3] W.A. Newcomb, Phys. Fluids B **3**, 1818 (1991).
[4] M.N. Rosenbluth and M.N. Bussac, Nucl. Fusion **19**, 489 (1979).
[5] C.W. Barnes *et al.*, Phys. Fluids **29**, 3415 (1986).
[6] T.R. Jarboe *et al.*, Phys. Fluids B **2**, 1342 (1990).
[7] J.H. Hammer *et al.*, Phys. Rev. Lett. **61**, 2843 (1988).
[8] J.H. Hammer *et al.*, Phys. Fluids B **3**, 2236 (1991).
[9] M.R. Brown and P.M Bellan, Phys. Rev. Lett. **64**, 2144 (1990).
[10] M.R. Brown and P.M. Bellan, Nucl. Fusion **32**, 1125 (1992).
[11] R. Raman *et al.*, Fusion Tech. **24**, 239 (1993).
[12] H. McLean, Lawrence Livermore National Laboratory (private communication).
[13] R. Décoste *et al.*, Plasma Phys. Controlled Nucl. Fusion Res. **1**, 383 (1992).
[14] K.M. McGuire *et al.*, Plasma Phys. Controlled Fusion Res. **30**, 1391 (1988).

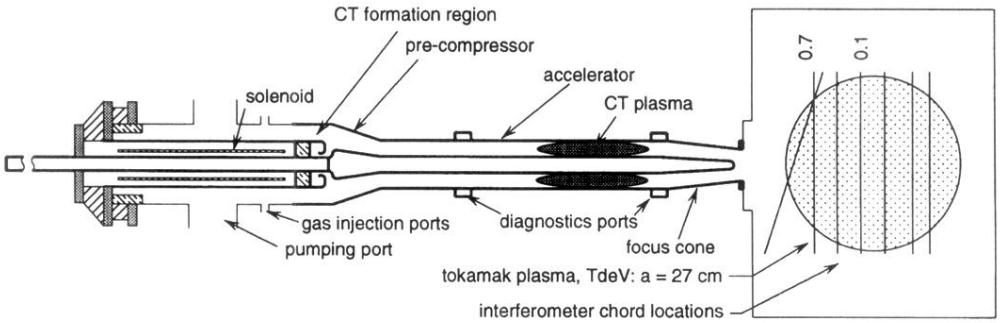

FIG. 1. Schematic of the experimental setup showing the CT injector in relation to the tokamak. The vertical lines overlaid on the tokamak cross section show the location of the interferometer beams. The $r/a = 0.1$ and 0.7 chords are located as shown in the figure.